PSFC/JA-04-36

Effects of hot electrons on the stability of a closed field line plasma

Krasheninnikova, Natalia S. and Catto, Peter J.

Plasma Science and Fusion Center
Massachusetts Institute of Technology
Cambridge, MA 02139 USA

Effects of hot electrons on the

stability of a closed field line plasma*

Natalia S. Krasheninnikova, Peter J. Catto

Massachusetts Institute of Technology, Plasma Science and Fusion Center

Cambridge, MA 02139

Abstract

Motivated by the electron cyclotron heating being employed on the dipole experiments, the effects of a hot species on stability in closed magnetic field line geometry are investigated by considering a Z-pinch plasma. The interchange stability of a plasma of background electrons and ions with a small fraction of hot electrons is considered. The species diamagnetic drift and magnetic drift frequencies are assumed to be of the same order, and the wave frequency is assumed to be much larger than the background, but much less than the hot drift frequencies. An arbitrary total pressure dispersion relation is obtained, with the background plasma treated as a single fluid, while a fully kinetic description is employed for the hot species. The analysis of the dispersion relation shows that two different kinds of resonant hot electron effects modify the simple MHD interchange stability condition. When the azimuthal magnetic field increases with radius, there is a critical pitch angle above which the magnetic drift of the hot electrons reverses. The interaction of the wave with the hot electrons with pitch angles near this critical value always results in instability. When the magnetic field decreases with radius, magnetic drift

reversal is not possible and only low speed hot electrons will interact with the wave. Destabilization by this weaker resonance effect can be avoided by carefully controlling the hot electron density and temperature profiles.

PACS numbers: 52.58.Lq, 52.55.Tn, 52.55.Hc.

I. INTRODUCTION

The Levitated Dipole Experiment (LDX)[1,2] is designed to operate in a magnetohydrodynamic (MHD) interchange stable regime[3-6]. Electron cyclotron heating is employed to increase the temperature[7] and will introduce a hot electron population that can alter interchange stability. We examine the effects of a hot Maxwellian electron population on interchange stability by considering a confined plasma having an ideal MHD background consisting of electrons and ions plus a fully kinetic population of hot electrons. Of particular interest is the role the hot electrons play in modifying the usual ideal MHD interchange stability condition by wave-particle resonance effects.

To simplify the analysis, we consider Z pinch geometry so that the unperturbed magnetic field B_0 is constant and closed on the cylindrical flux surfaces and the unperturbed diamagnetic current J_0 is along the axial direction. The Z pinch approximation to a dipole preserves the essential feature of the closed magnetic field lines, but misses the geometrical details associated with field line averages of quantities, so it is only intended to illustrate the key physics. A more realistic dipole equilibrium is required to make quantitative stability predictions. The Z-pinch model also allows us to consider plasmas in which the magnetic pressure is comparable to both the background kinetic pressure and the hot electron kinetic pressure, as well as to treat the diamagnetic and magnetic drifts as comparable as they are in a dipole. Moreover, it makes it possible to perform a kinetic treatment of the hot electron population in the limit in which the wave frequency resonates with the magnetic drift frequency to cause a destabilizing Landau-type resonance. In the low wave frequency limit of interest a particularly strong destabilizing hot electron interaction occurs when the hot electron magnetic drift exhibits reversal due to a change

in the grad B_0 direction. In the absence of drift reversal a much weaker resonant particle interaction can occur which can destabilize an otherwise stable interchange, with the new stability boundary depending on the details of the hot electron density, temperature and their profiles. To make the analysis more tractable and highlight the role of the hot electrons, only flute modes are considered with wave frequencies intermediate between the background and hot species drift frequencies. Flute or interchange modes are the least stable modes in the absence of hot electrons[3-6].

We note that the stability analysis presented here is completely different from those employed for a bumpy torus where a hot electron ring is necessary to provide stability in the otherwise unstable mirror cells linked to from a torus[8]. In a Z pinch model of a dipole, stability in the absence of hot electron is assured by employing a pressure profile that decreases slowly enough to satisfy the usual MHD interchange condition which arises due to the stabilizing influence of plasma and magnetic compressibility in closed magnetic field lines. The hot electrons generated by electron cyclotron heating must then be investigated to determine if they can act in a destabilizing manner. In particular, the curvature and grad B_0 drift must be treated on equal footing to allow a strongly unstable hot electron drift resonance to occur when the grad B_0 drift opposes the curvature drift (weaker destabilization occurs when the drifts are in the same direction). Here we remark that high mode number Z pinch interchange stability in the presence of hot electron population is in some details related to the low mode number alpha particle driven internal kink mode and fishbone instabilities in tokamaks. For these alpha particle driven modes the details of the resonance of the wave with the magnetic drift of the alphas can have a important impact, with drift reversal at some radius leading to instability[9]. In our Z pinch model we are able to investigate the resonant particle mechanism, in a simpler geometry that

allows us to give a physical interpretation of the effect of drift reversal, which occurs at some critical pitch angle (that is allowed to vary radially). These hot electron drift resonance effects are considered in detail in Sec. IV. In the electrostatic limit our results reduce to the standard hot electron interchange if hot electron temperature gradients are ignored and the hot electron density falls off radially[10].

In Sec. II we derive two coupled equations for the ideal MHD background plasma that depend on the perturbed hot electron number density and radial current. These two quantities are then evaluated kinetically in Sec. III assuming the unperturbed hot electron population is Maxwellian. Section IV combines the results from the two previous sections to obtain the full dispersion relation that is analyzed in detail, including the hot electron drift resonance de-stabilization effects. A simple hard core Z pinch geometry and the case of a "rigid rotor" are discussed in Sec. V. We close with a brief discussion of the results in Sec. VI.

II. IDEAL MHD TREATMENT OF THE BACKGROUND PLASMA

In this section we will develop an ideal MHD treatment for the background plasma that permits a hot electron population to be retained. This treatment allows us to derive a perturbed radial Ampere's law and a perturbed quasi-neutrality condition that depend on the perturbed hot electron radial current and density, respectively, which are evaluated in the next section.

We consider the simplest closed field line configuration of cylindrical Z-pinch geometry in which we only allow radial variation. The unperturbed magnetic field is in the azimuthal direction and given by $\vec{\mathbf{B}}_0 = B_0(r)\hat{\boldsymbol{\theta}}$, while the unperturbed current is axial and given by $\vec{\mathbf{J}}_0 = J_0(r)\hat{\mathbf{z}}$. Ampere's law requires

5

$$\mu_0 r J_0 = (r B_0)',$$ (1)

where a prime is used to denote radial derivatives.

Denoting the total equilibrium pressure by p_0, force balance gives

$$J_0 B_0 = -p_0',$$ (2)

where the total pressure is the sum of the background pressure, p_{0b} and hot pressure p_{0h}, $p_0 = p_{0b} + p_{0h}$. The background pressure $p_{0b} = p_{0e} + p_{0i}$ is the sum of the background electron pressure $p_{0e} = n_{0e} T_e$ and the ion pressure $p_{0i} = n_{0i} T_i$, where n_{0e}, n_{0i}, T_e, and T_i are the background electron and ion densities and temperatures. The total current is the sum of the background and hot contributions $J_0 = J_{0b} + J_{0h}$ which satisfy the force balance relations $J_{0b} B_0 = -p_{0b}'$ and $J_{0h} B_0 = -p_{0h}'$.

To derive the perturbed equations we linearize the full equations and assume the time and axial dependence are of the form $\exp(-i\omega t - ikz)$, with $\mathrm{Im}\,\omega > 0$ for an unstable mode. The background ion flow velocity $\vec{\mathbf{v}}_1$ is written in terms of the displacement $\vec{\xi}$ as $\vec{\mathbf{v}}_1 = -i\omega\vec{\xi}$. Making the usual ideal MHD assumption that the magnetic field moves with the flow, the perturbed electric field $\vec{\mathbf{E}}_1$ is

$$\vec{\mathbf{E}}_1 = i\omega\vec{\xi} \times \vec{\mathbf{B}}_0,$$ (3)

so that Faraday's law for the perturbed magnetic field $\vec{\mathbf{B}}_1$ becomes

$$\vec{\mathbf{B}}_1 = \nabla \times \left(\vec{\xi} \times \vec{\mathbf{B}}_0\right).$$ (4)

Knowing $\vec{\mathbf{B}}_1$, the total perturbed current $\vec{\mathbf{J}}_1 = \vec{\mathbf{J}}_{1b} + \vec{\mathbf{J}}_{1h}$ is evaluated from Ampere's law,

$$\mu_0 \vec{\mathbf{J}}_1 = \nabla \times \vec{\mathbf{B}}_1.$$ (5)

To determine the displacement we employ momentum conservation for the background plasma by accounting for the charge imbalance – or uncovering – due to the hot electrons:

$$-m_i n_{0i} \omega^2 \vec{\xi} = e n_{0h} \vec{E}_1 + \vec{J}_{1b} \times \vec{B}_0 + \vec{J}_{0b} \times \vec{B}_1 - \nabla p_{1b}, \tag{6}$$

where quasi-neutrality for singly charged ions requires $n_{0h} = n_{0i} - n_{0e}$ and m_i denotes the mass of the background ions. The perturbed pressure of the background plasma p_{1b} is assumed to satisfy an adiabatic equation of state

$$p_{1b} = -\gamma p_{0b} \nabla \cdot \vec{\xi} - p'_{0b} \xi_r, \tag{7}$$

where $\gamma = 5/3$ and ξ_r is the radial component of $\vec{\xi}$.

Using the preceding system of equations, it is convenient to obtain two coupled equations for the azimuthal component of $\vec{B}_1$ and the radial component of $\vec{\xi}$, that only require knowledge about the perturbed hot electron density and radial current which are evaluated in Sec. III. To carry out this simplification we first define the flux tube volume $V \equiv \oint dl / B_0 = 2\pi r / B_0$ and then form the $\hat{\theta}$ component of Eq. (4) to obtain

$$B_{1\theta} = \frac{V'}{V} B_0 \xi_r - B_0 \nabla \cdot \vec{\xi}, \tag{8}$$

with $V'/V = 1/r - B'_0/B_0$. Another useful expression is obtained from the radial component of Ampere's law, $ikB_{1\theta} = \mu_0 (J_{1br} + J_{1hr})$, by using the axial component of the momentum equation

$$-m_i n_{0i} \omega^2 \xi_z = e n_{0h} E_{1z} + B_0 J_{1br} + ik p_{1b}$$

to determine J_{1br}, then using Eq. (7) and the axial component of (3) to eliminate p_{1b} and $E_{1z} = i\omega B_0 \xi_r$, and finally using

$$\nabla \cdot \vec{\xi} = \frac{1}{r} \frac{\partial}{\partial r} (r\xi_r) - ik\xi_z \tag{9}$$

to eliminate ξ_z. Defining the background plasma beta by

$$\beta_b \equiv \frac{2\mu_0 p_{0b}}{B_0^2},$$ (10)

the resulting equation can be written as

$$B_{1\theta} = \frac{\mu_0 J_{1hr}}{ik} + \frac{\beta_b B_0}{2}\left\{\gamma\nabla\cdot\vec{\xi} + \left(\frac{p'_{0b}}{p_{0b}} - \frac{\omega e B_0 n_{0h}}{k p_{0b}}\right)\xi_r - \frac{\omega^2 m_i n_{0i}}{k^2 p_{0b}}\left[\nabla\cdot\vec{\xi} - \frac{1}{r}\frac{\partial}{\partial r}(r\xi_r)\right]\right\}.$$ (11)

If we neglect the coupling to sound waves by assuming $\omega^2/k^2 \ll p_{0b}/m_i n_{0i}$, use Eq.

(8) to eliminate $\nabla\cdot\vec{\xi}$, write ξ_r in terms of the axial electric field E_{1z}, and define the interchange

parameter

$$d = -\frac{V p'_{0b}}{V' p_{0b}}$$ (12)

and Maxwellian averaged background electron curvature and total magnetic drift frequencies

$$\omega_{\kappa e} = \frac{kT_e}{erB_0} \text{ and } \omega_{de} = \omega_{\kappa e}\frac{rV'}{V},$$ (13)

we obtain the first of the desired equations, the radial Ampere's law, in the form:

$$\left(1 + \frac{1}{2}\gamma\beta_b\right)\frac{B_{1\theta}}{B_0} = \frac{\mu_0 J_{1hr}}{ikB_0} + \frac{\beta_b}{2}\left[(\gamma - d)\frac{\omega_{de}}{\omega} - \frac{n_{0h}T_e}{p_{0b}}\right]\left(\frac{eE_{1z}}{ikT_e}\right).$$ (14)

Notice that in the absence of the hot electrons the sign of $B_{1\theta}$ changes at the marginal

interchange ideal MHD stability boundary $d = \gamma$.

To obtain the second equation we start with background charge conservation

$\nabla\cdot\vec{J}_{1b} = i\omega e(n_{1i} - n_{1e})$ and use perturbed quasi-neutrality $n_{1h} = n_{1i} - n_{1e}$ to write

$$i\omega e n_{1h} = \nabla\cdot\vec{J}_{1b}.$$ (15)

8

The interchange assumption means that only the perpendicular component of $\vec{J}_{1b}$ matters in Eq. (15). Solving the momentum equation for $\vec{J}_{1b\perp}$ by making sure to retain the inertial term in J_{1bz} but continuing to ignore it in J_{1br}, and inserting the result into Eq. (15), gives

$$i\omega e \left[n_{1h} + \left(n'_{0h} + \frac{\omega k n_{0i} m_i}{eB_0} \right) \xi_r + n_{0h} \nabla \cdot \vec{\xi} \right] = -ik \left(\frac{p_{1b} V'}{B_0 V} + \frac{p'_{0b} B_{1\theta}}{B_0^2} \right).$$

Using Eqs. (7) and then (8) to eliminate p_{1b} and then $\nabla \cdot \vec{\xi}$, writing ξ_r in terms of E_{1z}, using definitions (12) and (13), and defining $\Omega_i = eB_0 / m_i$ and

$$b = \frac{k^2 T_e}{m_i \Omega_i^2} \frac{n_{0i} T_e}{p_{0b}}, \tag{16}$$

the preceding gives the quasi-neutrality equation, to be

$$\frac{n_{1h} T_e}{p_{0b}} + \left[b + \frac{\omega_{de}}{\omega} \frac{n_{0h} T_e}{p_{0b}} \left(1 + \frac{r n'_{0h} / n_{0h}}{r V' / V} \right) - \frac{\omega_{de}^2}{\omega^2} (\gamma - d) \right] \left(\frac{e E_{1z}}{ik T_e} \right) = \frac{B_{1\theta}}{B_0} \left[\frac{n_{0h} T_e}{p_{0b}} - \frac{\omega_{de}}{\omega} (\gamma - d) \right]. \tag{17}$$

Combining Eqs. (14) and (17) in the absence of hot particles we recover the usual arbitrary β_b ideal MHD interchange condition[5] in the form

$$\left(\frac{\omega}{\omega_{\kappa e}} \right)^2 = \left(\frac{r V'}{V} \right)^2 \frac{(\gamma - d)}{b} \frac{(2 + d\beta_b)}{(2 + \gamma\beta_b)}. \tag{18}$$

Notice that since our MHD treatment requires $b \ll 1$ and we are interested in $d \sim 1$, the frequency range of interest is $\omega \gg \omega_{\kappa e}$ as assumed. The same coupled system of equations (14) and (17) can also be obtained kinetically following a procedure which assumes the transit frequency is much greater than the collision frequency which is much greater than the wave, magnetic drift and diamagnetic frequencies[11]. To analyze the modifications due to a Maxwellian hot electron population, n_{1h} and J_{1hr} are calculated kinetically in the next section.

III. KINETIC TREATMENT OF THE HOT ELECTRONS

To complete our description we need to kinetically evaluate the perturbed hot electron density and radial current contribution to the Ampere's law and quasi-neutrality equations (14) and (17). The hot electron response must be evaluated kinetically since the temperature of the hot electron population, T_h, is assumed to be much larger that the background temperatures. As a result, the magnetic drift and diamagnetic frequencies of the hot electrons will be assumed to be much larger than the wave frequency.

We assume that the hot electrons satisfy the Vlasov equation. We then linearize by assuming the unperturbed hot electron distribution function, f_{0h}, is a hot Maxwellian plus a diamagnetic correction:

$$f_{0h} = f_{Mh} - \Omega_e^{-1} \vec{v} \times \hat{\mathbf{\theta}} \cdot \nabla f_{Mh}, \tag{19}$$

where $f_{Mh} = n_{0h}(m_e / 2\pi T_h)^{3/2} \exp(-m v^2 / 2T_h)$ and $\Omega_e = eB_0 / m_e$, with m_e the electron mass.

The gyro-kinetic equation for the linearized hot electron distribution function f_{1h} is most conveniently rewritten by introducing the scalar and vector potentials via $\vec{\mathbf{E}}_1 = -\nabla \Phi - \partial \vec{\mathbf{A}} / \partial t$ and $\vec{\mathbf{B}}_1 = \nabla \times \vec{\mathbf{A}}$, extracting the adiabatic response by letting

$$f_{1h} = \frac{e\Phi_1}{T_h} f_{Mh} + g e^{iL}, \tag{20}$$

where $L = \Omega_e^{-1} \vec{\mathbf{k}} \cdot \vec{v} \times \hat{\mathbf{\theta}}$ and $\vec{v} = v_\perp (\hat{\mathbf{z}}\cos\theta + \hat{\mathbf{r}}\sin\theta) + v_\parallel \hat{\mathbf{\theta}}$, and then seeking solutions of the form $\exp(-i\omega t - iS)$ where $\nabla S = \vec{\mathbf{k}}_\perp$. The resulting gyro-kinetic equation for g becomes[12,13]

$$-i(\omega - \vec{\mathbf{k}} \cdot \vec{v}_{dh})g = i\frac{e}{T_h} f_{Mh}(\omega - \omega_{*h}^T)\left[(\Phi - v_\parallel A_\theta)J_0(a_h) - \frac{v_\perp B_{1\theta}}{k_\perp} J_1(a_h)\right], \tag{21}$$

where $a_h = k_\perp v_\perp / \Omega_e$. In Eq. (21)

$$\vec{\mathbf{k}} \cdot \vec{\mathbf{v}}_{dh} = \frac{k}{r\Omega_e}\left(v_\parallel^2 - v_\perp^2 \frac{rB_0'}{2B_0}\right) = \omega_{\kappa h} \frac{mv^2}{2T_h}\left[(1+s)\lambda^2 + (1-s)\right] \qquad (22)$$

is the grad B_0 plus curvature magnetic drift frequency with $\omega_{\kappa h} = kT_h/erB_0$ the curvature drift

frequency, $\lambda = v_\parallel/v$ a pitch angle variable and

$$s \equiv 1 + \frac{rB_0'}{B_0}, \qquad (23)$$

where $s = 0$ corresponds to the vacuum limit. In addition,

$$\omega_{*h}^T = \omega_{*h}\left[1 + \eta_h\left(\frac{mv^2}{2T_h} - \frac{3}{2}\right)\right] \qquad (24)$$

is the hot electron diamagnetic drift frequency with $\eta_h = (T_h'/T_h)/(n_{0h}'/n_{0h})$ and

$$\omega_{*h} = -\frac{kT_h n_{0h}'}{eB_0 n_{0h}}. \qquad (25)$$

The $v_\parallel/(\omega - \vec{\mathbf{k}} \cdot \vec{\mathbf{v}}_{dh})$ moment of the gyro-kinetic equation (21) shows that $J_{1\theta h}$ is

proportional to A_θ. Moreover, there is no perturbed parallel current carried by the background

plasma. As a result, the parallel component of the Ampere's law results in a homogeneous

equation for A_θ. Therefore, we may safely assume $A_\theta = 0$ and $\vec{\mathbf{B}}_1 = B_{1\theta}\hat{\theta}$. In addition, we

assume that axial wavelengths are much shorter than azimuthal wavelengths and radial

derivatives of unperturbed quantities. Consequently, $k_\perp \approx k$, $L \approx kv_\perp\Omega_e^{-1}\sin\theta$ and

$a_h \approx kv_\perp/\Omega_e$ may be employed. Finally, we allow hot to background temperature ratio to be as

large as $T_h/T_e \sim m_i/m_e$ so that $a_h^2 \sim b \ll 1$ and $L \ll 1$. Then we may use $J_0 \approx 1$, $J_1 \approx a_h/2$,

and $\exp(iL) \approx 1 + iL$ to reduce Eqs. (20) and (21) to

$$f_{1h} \approx f_{Mh}\left[\frac{e\Phi}{T_h} - \left(\frac{\omega - \omega_{*h}^T}{\omega - \vec{\mathbf{k}} \cdot \vec{\mathbf{v}}_{dh}}\right)\left(\frac{e\Phi}{T_h} - \frac{mv_\perp^2 B_{1\theta}}{2T_h B_0}\right)(1 + iL)\right]. \qquad (26)$$

11

To simplify our calculations, we note that our short axial wavelength assumption along with the Coulomb gauge $\nabla \cdot \vec{\mathbf{A}} = 0$ implies that $A_z \ll A_r$. As a result, $E_{1z} \approx ik\Phi$ may be employed to make the replacement

$$\frac{eE_{1z}}{ikT_e} \approx \frac{e\Phi}{T_e}. \tag{27}$$

in perturbed radial Ampere's law, Eq. (14) and quasi-neutrality condition, Eq. (17). If the assumption of $\beta_b \sim 1$ is made, these equations also imply the ordering

$$\frac{B_{1\theta}}{B_0} \sim \frac{e\Phi\omega_{\kappa e}}{T_e\omega} = \frac{e\Phi\omega_{\kappa h}}{T_h\omega}. \tag{28}$$

To simplify the results for the hot electrons while maintaining $T_h \gg T_e$ we will assume $\omega_{\kappa h} \gg \omega \gg \omega_{\kappa e}$ and thus

$$\frac{T_h}{T_e} \gg \frac{\omega}{\omega_{\kappa e}} \gg 1. \tag{29}$$

Keeping the above simplifications in mind, we can integrate the distribution function, Eq. (26), over velocity space and obtain perturbed hot electron density, $n_{1h} = \int f_{1h} d\vec{\mathbf{v}}$, and radial current, $J_{1hr} = -e\int \mathrm{v}_r f_{1h} d\vec{\mathbf{v}}$. Fortunately, the full expressions for n_{1h} and J_{1hr} will not be required. Only the approximations given in the Appendix are needed. For the moment we need only define the hot electron beta

$$\beta_h = \frac{2\mu_0 p_{0h}}{B_0^2} \quad \text{and} \quad s_h = -\frac{\beta_h}{2}\frac{rp'_{0h}}{p_{0h}},$$

and comment that the expressions in the Appendix lead to the forms:

$$\frac{n_{1h}}{n_{0h}} = \frac{e\Phi}{T_h}G + \frac{B_{1\theta}}{B_0}H \quad \text{and} \quad \frac{\mu_0 J_{1hr}}{ikB_0} = \frac{e\Phi_1}{T_h}\frac{\beta_h}{2}H - \frac{B_{1\theta}}{B_0}s_h I, \tag{30}$$

where $H \sim G \sim s_h I \sim 1$, except in the vicinity of $s = 1$, where $H \sim G \sim s_h I \sim \sqrt{\omega_{\kappa h}/\omega}$. We remark that even though $\omega_{\kappa h} \gg \omega$, it is important to keep the ω term in the denominator of the f_{1h} expression to resolve singularities during the evaluation of the integrals.

IV. DISPERSION RELATION

Combining the perturbed radial Ampere's law, Eq. (14), and quasi-neutrality condition, Eq. (17), with the expressions for n_{1h} and J_{1hr} from the previous section, we can form the dispersion relation, which can be written as

$$
\begin{aligned}
&\left\{ b + \frac{\omega_{de}^2}{\omega^2}(d - \gamma) + \frac{n_{0h}T_e}{p_{0b}}\left[\frac{T_e}{T_h}G + \frac{\omega_{de}}{\omega}\left(1 + \frac{rn'_{0h}/n_{0h}}{rV'/V}\right) \right] \right\}\left(1 + \tfrac{1}{2}\gamma\beta_b + s_h I\right) + \\
&+ \frac{\beta_b}{2}\left[\frac{\omega_{de}}{\omega}(d - \gamma) + \frac{n_{0h}T_e}{p_{0b}}(1 - H)\right]^2 = 0
\end{aligned}
\tag{31}
$$

If we consider comparable hot electron pressure and background pressure then in the absence of the finite Larmor radius term b, Eq. (31) is seen to permit only solutions with $\omega_{de}/\omega \sim n_{0h}/n_{0i}$ since we order $d \sim \beta_b \sim \beta_h \sim s_h I \sim G \sim H \sim V n'_{0h}/n_{0h}V'$ for the case of $s \neq 1$. Therefore, the neglect of b violates the ordering imposed by Eq. (29) when $\beta_b \sim \beta_h$. Consequently we proceed for now by assuming $b \sim \omega_{\kappa e}^2/\omega^2 \gg (n_{0h}/n_{0i})^2$ and neglecting order $n_{0h}/n_{0i} \sim T_e/T_h$ terms compared to $\omega_{\kappa e}/\omega$ in the dispersion relation. For the case of $s \neq 1$ this assumption corresponds to neglecting G and H as well as the equilibrium hot electron density gradient term. Thus, the only hot electron contribution that matters in Eq. (31) is $s_h I$ and the dispersion relation then reduces to

$$\frac{\omega^2}{\omega_{\kappa e}^2} = \left(\frac{rV'}{V}\right)^2 \frac{(\gamma-d)}{b} \frac{\left(1+\frac{1}{2}d\beta_b+s_hI\right)}{\left(1+\frac{1}{2}\gamma\beta_b+s_hI\right)} . \tag{32}$$

Had we retained finite hot electron gyro-radius terms they would have entered as small order a_h^2

corrections to $s_h I$ in Eq. (32).

To evaluate I we only need the lowest order expression for J_{1hr} :

$$\frac{\mu_0 J_{1hr}}{ikB_0} \approx -\frac{\beta_h B_{1\theta}\omega_{*h}}{\sqrt{\pi}B_0\omega_{\kappa h}} \int_0^\infty dt\, e^{-t^2} t^4 \left[1+\eta_h\left(t^2-\frac{3}{2}\right)\right]\int_{-1}^{1} \frac{d\lambda\left(1-\lambda^2\right)^2}{D-\omega/\omega_{\kappa h}t^2} = -\frac{B_{1\theta}}{B_0}s_h I , \tag{33}$$

where $t^2 = m\mathrm{v}^2/2T_h$ and $D = (1+s)\lambda^2 + (1-s)$. To perform the integral in I we may neglect

the ω term by using $\omega << \omega_{\kappa h}$ in the denominator except (i) in the vicinity of $s=1$ and (ii) to

insure the path of integration is on the causal side of the $D=0$ singularity for $s>1$. Leaving the

details of this calculation to the Appendix, we find that we can write the expression for I as

$$I \approx \begin{cases} -\frac{1}{(1+s)^2}\left((s+4)+\frac{3}{\sqrt{s^2-1}}\ln\left(s+\sqrt{s^2-1}\right)-\frac{3\pi i}{\sqrt{s^2-1}}\right) & s>1 \\[2ex] -\left[\frac{5}{4}-i\sqrt{\frac{\omega_{\kappa h}}{\omega}}\frac{\sqrt{2\pi}\left(1+\frac{3}{2}\eta_h\right)}{(1+\eta_h)}\right] & s=1 \\[2ex] -\frac{1}{(1+s)^2}\left((s+4)-\frac{6}{\sqrt{1-s^2}}\arctan\sqrt{\frac{1+s}{1-s}}\right) & -1<s<1 \\[2ex] \frac{2}{5} & s=-1 \\[2ex] -\frac{1}{(1+s)^2}\left((s+4)-\frac{3}{\sqrt{s^2-1}}\ln\left(-s+\sqrt{s^2-1}\right)\right) & s<-1 \end{cases} \tag{34}$$

Expressions for I in the vicinity of $s=1$ are given in the Appendix for completeness. We

remark that our analysis ignores drift resonances of the background species since they are

exponentially small and of order $\exp(-\omega_0/\omega_{\kappa e})$, where $\omega_0 >> \omega_{\kappa e}$.

Notice that for $s>1$ a large imaginary term enters because of the vanishing of the hot

electron drift velocity for some pitch angle. This singularity in the drift introduces a Landau

resonance in pitch angle space between the wave and the drifting hot electrons. The effective dissipation associated with the vanishing of the hot electron drift resonance makes it such that stable solutions are no longer possible because one of the roots will always have $\text{Im}\,\omega > 0$. Before examining the $s < 1$ case in detail we discuss the physical mechanism responsible for instability when $s \gtrsim 1$.

The Landau resonance between the wave and the hot electron magnetic drift has two different forms. When $s < 1$ the hot electron magnetic drift does not reverse and the wave-particle interaction is weak because the wave frequency is much smaller than the hot electron drift frequency except for a very low speed hot electrons. That is $\omega = \vec{\mathbf{k}} \cdot \vec{\mathbf{v}}_{dh}$ can only be satisfied if v is very small since the surfaces of constant $\vec{\mathbf{k}} \cdot \vec{\mathbf{v}}_{dh}$ are closed ellipses about $\mathrm{v} = 0$ in the $\mathrm{v}_{\parallel}, \mathrm{v}_{\perp}$ plane. As s approaches unity the ellipse opens and becomes hyperbolic because the drift frequency reverses. A stronger interaction occurs for $s \geq 1$ because particles of all speed are resonant near the critical pitch angle. For $s > 1$ the hot electrons with smaller pitch angles drift along the negative z axis while the larger pitch angle ones continue to drift in the positive z direction. The energy exchange with the near stationary wave is strong since many more hot electrons are involved in the resonant interaction.

For the special case $s = 1$ there is only curvature drift and all hot electrons are drifting in the same direction along the positive z axis. Energy flows from these particles to the nearly stationary growing wave since all the particles are moving faster than the wave and are therefore being slowed by it. As s increases above unity the drift direction of the lower pitch angle hot electrons reverse and these hot electron moving slower than the wave are able to extract energy from it so the growth rate decreases. The wave remains unstable, however, because of the

parabolic dependence of the magnetic drift on pitch angle, $\vec{\mathbf{k}} \cdot \vec{\mathbf{v}}_{dh} \propto \lambda^2 - \lambda_0^2$ with $\lambda_0^2 = (s-1)/(s+1)$. This dependence means that a typical hot electron with $\lambda = \lambda_0 + \delta$ is moving faster than a typical one with $\lambda = \lambda_0 - \delta$, that is,

$$\left| \frac{\vec{\mathbf{k}} \cdot \vec{\mathbf{v}}_{dh}\big|_{\lambda=\lambda_0+\delta}}{\vec{\mathbf{k}} \cdot \vec{\mathbf{v}}_{dh}\big|_{\lambda=\lambda_0-\delta}} \right| = \frac{2\lambda_0+\delta}{2\lambda_0-\delta} > 1 .$$

As a result, the $s > 1$ case is always unstable since the hot electrons with pitch angles above the critical pitch angle for drift reversal, λ_0, are always able to give more energy to the wave than those below λ_0, which extract it from the wave. Because a Maxwellian is independent of pitch angle, there are equal numbers of slightly faster and slower hot electrons within δ of λ_0. Because $\omega << \omega_{\kappa h}$, the wave is essentially stationary and simply a means of transferring energy between the counter drifting hot electrons so ω may safely be neglected in the expressions for I (except near $s = 1$ where I depends on ω because there are few if any drift reversed particles). Only in the limit $s \to \infty$, when the drifts of all hot electrons are reversed does the resonant drive vanish for $s \geq 1$.

The special case $rV'/V = 2 - s \to 0$ corresponds to $B_0 \propto r$ (flux tube volume independent of r), but since $d \propto V/rV' \to \infty$ it is always unstable even in the absence of hot electrons as can be seen from Eq. (32). The growth rate ($\mathrm{Im}\,\omega$) for other $s > 1$ can be estimated from Eqs. (32) and (34) to find

$$\mathrm{Im}\,\omega/\omega_{\kappa e} \sim \beta_h \beta_b |\gamma - d|^{3/2} |2 - s| \Big/ \sqrt{b|s^2 - 1|} \tag{35}$$

for $\beta_b \sim d \sim 1$. Notice that the growth rate vanishes for $d = \gamma$ and/or $s \to \infty$.

For $s < 1$ the stable operating regime of most interest satisfies the usual interchange stability condition $\gamma > d$ along with the additional condition $1 + \beta_b d / 2 + s_h I > 0$. To better understand this regime it is convenient to write equilibrium force balance in terms of s as $s + (\beta_b + \beta_h) r p_0' / (2 p_0) = 0$. Then d can be written in terms of s and s_h as

$$1 + \tfrac{1}{2} \beta_b d = \tfrac{2 - s_h}{2 - s} . \tag{36}$$

Using this result, $\gamma > d$ becomes

$$s_h > -\gamma \beta_b + \left(1 + \tfrac{1}{2} \gamma \beta_b\right) s . \tag{37}$$

Then, ignoring for the moment resonant particles effects for $s < 1$, the stability condition of Eq. (32) can be illustrated graphically by plotting s_h as a function of s for a given value of background beta as shown in Figs. 1.

Notice that when the hot electrons are ignored, i.e. $s_h = 0$, we recover the usual Z-pinch stability condition[14], $s < \gamma \beta_b / (1 + \gamma \beta_b / 2)$. The plots also show that the β_b term increases the size of the stable region, allowing more general hot pressure profiles (i.e. s_h can be negative as well as positive for $s = 0$). However, as $s \rightarrow 1$, I becomes large, so the curves $1 + d\beta_b / 2 + s_h I = 0$ and $1 + \gamma \beta_b / 2 + s_h I = 0$, which cross at $d = \gamma$, require $s_h \rightarrow 0$ at $s = 1$. To prevent a sign change in Eq. (32) we need to be above all three curves to maintain stability. From plots like Figs. 1 we can see that a value of $\gamma \beta_b$ between about 3 and 5 optimizes the stable operating region since a larger β_b does not substantially increase the stable operating regime.

So far we have assumed $|r n_{0h}' / n_{0h}| \sim 1$ and thus, due to Eq. (29), were able to neglect terms that involve hot electron density gradient. However, it is possible to have a steeper hot electron density gradient – so steep that $|r n_{0h}' / n_{0h}| \gg 1$. If we assume that the hot electron

temperature and density profiles are similar and consider a smooth profile for equilibrium background pressure, then $\left|rn'_{0h}/n_{0h}\right| \sim \left|s_h\right| \sim \left|s\right|$ due to equilibrium force balance, $s = -\beta_b rp'_{0b}/2p_{0b} + s_h$. However the hot electron density gradient only enters in the form $(rn'_{0h}/n_{0h})/(2-s)$, which for $\left|rn'_{0h}/n_{0h}\right| \gg 1$ is of order unity. Thus because of the direct relation between $\left|rn'_{0h}/n_{0h}\right|$ and $\left|s\right|$ through the equilibrium force balance and the ordering imposed by Eq. (29), the hot electron density gradient terms will never become significant enough to appear in the dispersion relation.

During the operation of LDX it is anticipated that the hot electron pressure will become much larger than background pressure. Therefore we also consider the case of $\beta_h \gg \beta_b$, by taking $b \sim \omega_{\kappa e}^2/\omega^2 \sim (n_{0h}/n_{0i})^2$. This ordering leads to neglecting only the G term in the lowest order dispersion relation Eq. (31), due to the ordering imposed by Eq. (29).

As before, the drift reversal case $(s > 1)$ continues to be strongly destabilizing due to large imaginary terms in I and H. If we ignore weak resonant hot electron effects, the stability condition for $s < 1$ case can be written as

$$1 + Y \geq 0, \tag{38}$$

where to the lowest order we find $H = -\frac{rn'_{0h}}{2n_{0h}} \int_{-1}^{1} \frac{d\lambda(1-\lambda^2)}{(1+s)\lambda^2+(1-s)}$ from Eq. (A7), and we define

$$Y = \frac{2(\gamma-d)}{\left(1+\frac{rn'_{0h}/n_{0h}}{rV'/V}\right)^2}\left[\frac{2b}{(n_{0h}T_e/p_{0b})^2}\frac{\left(1+\frac{1}{2}d\beta_b+s_hI\right)}{\left(1+\frac{1}{2}\gamma\beta_b+s_hI\right)} - \frac{\beta_b(1-H)\left(\frac{rn'_{0h}/n_{0h}}{rV'/V}+H\right)}{\left(1+\frac{1}{2}\gamma\beta_b+s_hI\right)}\right].$$

If electrostatic fluctuations are considered (i.e. $\beta_b = 0$ and $s = 0$) this condition reduces to

$$\left(\frac{n_{0h}T_e}{p_{0b}}\right)^2\left(1+\frac{rn'_{0h}/n_{0h}}{rV'/V}\right)^2 + 4b(\gamma-d) \geq 0,$$

from which we can see that electrostatically the hot electrons improve lowest order stability by allowing d to be larger than γ since $b > 0$.

Examining the full expression for $Y + 1$ we see that when $\beta_b \rightarrow 0$, $Y \gg 1$ since $\beta_b d = 2(s - s_h)/(2 - s) \sim 1$. As a result, the stability boundaries are the same as in Fig. 1(a) for this limit. For other values of β_b, the stability regions can be plotted as shown in Figs. 2 for various values of $\gamma \beta_b$ and rn'_{0h}/n_{0h}. Comparing Figs. 2 (a),(b) with Fig. 1 (b) and Figs. 2 (c),(d) with Fig. 1 (c) we can see that the hot electrons somewhat improve the lowest order stability, as in the electrostatic limit.

Comparing the plots of Figs. (1) and (2) we can conclude that stability remains robust even at $\beta_h \gg \beta_b$ as long as the region of operation is above the solid curves and the area of drift reversal ($s > 1$) is avoided, with higher hot electron fractions improving stability.

As noted earlier, the resonant hot electron interaction enters as a weaker effect for $s < 1$ than it does for $s > 1$, which is always strongly unstable. We next consider the effect of these resonant hot electrons on stability for $s < 1$ by evaluating their contributions to the perturbed hot electron density and radial current density for the real part of ω greater than zero ($\operatorname{Re}\omega > 0$) as described in the Appendix:

$$\left.\frac{n_{1h}}{n_{0h}}\right|_{res} = \frac{B_{1\theta}}{B_0}H_{res} + \frac{e\Phi}{T_h}G_{res} \quad \text{and} \quad \left.\frac{\mu_0 J_{1hr}}{ikB_0}\right|_{res} = \frac{e\Phi_1}{T_h}\frac{\beta_h}{2}H_{res} - \frac{B_{1\theta}}{B_0}\left(s_h I\right)_{res}, \qquad (39)$$

where

$$G_{res} = -i\Delta\frac{15\beta_b}{\beta_h}\left(\frac{T_h}{T_e}\right)^2$$

$$H_{res} = -\frac{2\omega_0 G_{res}}{3\omega_{\kappa h}(1-s)} \quad \text{and} \quad \left(s_h I\right)_{res} = -\frac{4\beta_h\omega_0^2 G_{res}}{15\omega_{\kappa h}^2(1-s)^2} \qquad (40)$$

with Δ defined by

$$\Delta = \frac{(2\pi\omega_0)^{1/2} \, \omega_{*h} \left(1 - \frac{3}{2}\eta_h\right)}{15\omega_{\kappa h}^{3/2}(1-s)} \frac{\beta_h}{\beta_b}\left(\frac{T_e}{T_h}\right)^2 . \tag{41}$$

Here and elsewhere ω_0 is the positive stable root of Eq. (31), which can be schematically represented as

$$A \frac{\omega_0^2}{\omega_{de}^2} + B \frac{\omega_0}{\omega_{de}} + C = 0 ,$$

where A, B and C are coefficients of corresponding powers of ω_0 / ω_{de}.

Retaining the resonant interaction perturbatively in Eq. (31) using $\omega = \omega_0 + \omega_1$, with $\omega_0 \gg |\omega_1|$ gives

$$\frac{\omega_1}{\omega_0} = i\Delta K F , \tag{42}$$

where

$$K = \left\{ \kappa[1 - \alpha(1-H)] - \frac{5/2}{\left(1 + H\frac{\alpha}{1-\alpha}\right)} \right\}^2 + \frac{25}{4}\left[\frac{6}{5} - \frac{1}{\left(1 + H\frac{\alpha}{1-\alpha}\right)^2}\right] = \\ = \kappa^2[1 - \alpha(1-H)]^2 - 5\kappa(1-\alpha) + \frac{15}{2} \tag{43}$$

and

$$F = \frac{\left(1 + \frac{1}{2}\gamma\beta_b + s_h I\right)}{A + \frac{\omega_{de}}{2\omega_0}B} , \tag{44}$$

with

$$\kappa = \frac{\beta_b(\gamma - d)(2-s)}{\left(1 + \frac{1}{2}\gamma\beta_b + s_h I\right)(1-s)} \quad \text{and} \quad \alpha = \frac{\omega_0 n_{0h} T_e}{\omega_{de} p_{0b}(\gamma - d)} . \tag{45}$$

If we consider comparable background and hot electron pressures ($\beta_h \sim \beta_b$), then the α terms become negligible because using Eq. (32) gives $\alpha \sim n_{0h}T_e / \left(p_{0b}\sqrt{b}\right) \ll 1$. After

substituting in the expressions for A and B in this limit, we find that $F = 1$ and Eq. (42) then reduces to

$$\frac{\omega_1}{\omega_0} = \frac{i\Delta}{b}\left[\left(\kappa - \frac{5}{2}\right)^2 + \frac{5}{4}\right],$$

(46)

As we can see the sign of ω_1 / ω_0 depends only on the sign of Δ. As a result, for $\beta_h \sim \beta_b$, a weak instability of the drift resonant hot electrons ($\omega_0 > 0$) occurs if $\omega_{*h}(1 - 3\eta_h / 2) > 0$ or

$$\frac{3}{2}\frac{rT_h'}{T_h} > \frac{rn_{0h}'}{n_{0h}}.$$

(47)

Notice that in the electrostatic limit $\beta_b = 0$, so that $\kappa = 0$ making K positive as well as $F = 1$. As a result, instability is still determined by the sign of Δ and therefore by Eq. (47). It is also clear that temperature profile of hot electrons plays an important role in stabilizing this weak drift instability, since if $\eta_h = 0$ only increasing density profiles can be stable. To confirm that this drift resonance driven mode is indeed weak for $s < 1$ we note that $(\omega_0 / \omega_{\kappa e})^2 \sim 1/b$ giving $\omega_1 / \omega_0 \sim (\beta_h / \beta_b)(\omega_0 / \omega_{\kappa h})^{5/2} << 1$ for $\beta_h \sim \beta_b$.

The analysis of weak resonant hot electrons effects for the case of $\beta_h >> \beta_b$ is more complicated since the stability is determined by the full Eq. (42). We first observe that we are only interested if the stable operating region above the solid curve in Figs. (2) can become destabilized by this weak interaction, since the stable region below the solid curve does not allow the hot electron pressure to fall off (positive s_h). In the region of interest, above the solid curve in Figs. (2), the numerator of F is clearly positive, while the denominator is also positive, but for a more subtle reason. Since the negative real roots of the dispersion relation Eq. (31) are always stable in the absence of resonant hot electrons we are only interested in $\omega_0 > 0$. Using

our schematic representation of zero order dispersion relation the denominator of F can be rewritten as

$$A + \frac{\omega_{de}}{2\omega_0}B = \pm \frac{\omega_{de}}{2\omega_0}\sqrt{B^2 - 4AC} \ .$$

In the region of interest $AC < 0$ and $A > 0$, thus the dispersion relation has two real roots – one positive and one negative. Only positive root can be unstable, and it makes the denominator of F positive. Consequently, the sign of ω_1 / ω_0 depends on the sign of the product of Δ and K.

In the region of interest $d < \gamma$, and therefore $\alpha, \kappa > 0$. If $\alpha > 1$ then K is positive. If $0 < \alpha < 1$ and $H > 0$ (i.e. $rn'_{0h} / n_{0h} < 0$) then $1 + H\alpha/(1-\alpha) > 1$ and K is again positive. So for these two cases the stability is determined only by the sign of Δ and is identical to $\beta_h \sim \beta_b$ case, Eq. (46). However, when $rn'_{0h} / n_{0h} > 0$ and thus $H < 0$, the sign of K can become negative so stability depends on the sign of its product with Δ. For the general case, the stability boundary has to be obtained numerically. However, if $b << (n_{0h}T_e / p_{0b})^2$ and $Y << 1$ then a simple condition, that approximates the stability boundary can be found by substituting the expression for ω_0 in the form

$$1 - \alpha + \alpha H \approx \frac{\tau + H}{(\tau + 1)^2} \tag{48}$$

into Eq. (43). Solving $K = 0$ for s_h yields the approximation to the left side of the stability boundary given by

$$s_h = \frac{\left(1 + \frac{1}{2}\gamma\beta_b\right)[2(2-s) - x(1-s)] - 4}{[xI(1-s) - 2]} \tag{49}$$

with

$$x = \frac{5\tau(1+\tau)}{2(\tau+H)^2}\left[1 \pm \sqrt{1 - \frac{6(\tau+H)^2}{5\tau^2}}\right] \qquad \text{and} \qquad \tau = \frac{rn'_{0h} / n_{0h}}{2-s},$$

and where H is proportional to rn'_{0h}/n_{0h} and given after Eq. (38). In this $b=0$ limit Y reduces to

$$Y \approx -2\kappa\alpha \frac{(1-H)[1-\alpha(1-H)](1-s)}{(2-s)}.$$

From this form of Y we can see that $Y \ll 1$ requires either small κ (or $\beta_b \ll 1$) or small $1-\alpha+\alpha H$, which from Eq. (48) requires large rn'_{0h}/n_{0h}. Assuming $rn'_{0h}/n_{0h} \gg 1$ and using Eq. (48) we expect that Eq. (49) is adequate when

$$Y \approx -\frac{2\kappa(\tau+H)(1-s)}{\tau^2(2-s)} \sim \frac{\beta_b}{rn'_{0h}/n_{0h}} \ll 1.$$

For $rn'_{0h}/n_{0h} > 0$ the plot of stability regions is given in Figs. 3 for $b=0$ and $b=0.01$ for different values of $\gamma\beta_b$ and rn'_{0h}/n_{0h}. The faint grey curves show the zero order stability boundaries of Fig. 2. In Fig. 3 (a) and (c) only the stability boundary for $b=0.01$ is shown, since for the special case of $b \ll (n_{0h}T_e/p_{0b})^2$ and $Y \ll 1$ the $s_h > 0$ region is stable. In Figs. 3 (b) and (d) the dash-dotted line is the $b=0$ case, while the $b=0.01$ case is the solid line. We also plot the analytical approximation of Eq. (49) to the boundary for the $b=0$ case to show its good agreement with the numerical calculation. We do not plot the analytical solution in Fig. 3 (d) since the agreement is so good, it becomes impossible to tell two curves apart.

We find from plots like Figs. 3 that for $b \ll (n_{0h}T_e/p_{0b})^2$ and $Y \ll 1$ the analytical solution, Eq. (49) approximates the left side of the stability boundary very well. However, as the hot electron density gradient drops the approximation becomes invalid. It is also clear by examining plots like Fig. 3 (b) or (d) that high hot electron fractions satisfying $b \sim (n_{0h}T_e/p_{0b})^2$ make the unstable region the largest. Consequently, for our $b \ll 1$ ordering, large hot electron fractions are desirable. Comparing Fig. 3 (a) and (d) we can conclude that while large hot

electron density gradient as well as high background beta are beneficial for the zero order stability, they are destabilizing when the first order correction is considered if rn'_{0h}/n_{0h} is positive and greater than 2-3 for $\beta_b \sim 1$. If the density gradient is small, then higher $\gamma\beta_b$ operation becomes possible, Moreover, if $\gamma\beta_b$ is small (the electrostatic limit) then the zero order stability region is reduced and does not permit appreciable positive hot pressure gradients ($s_h > 0$). Thus to maximize the overall stable region $rn'_{0h}/n_{0h} > 0$, it is best to keep $\gamma\beta_b \sim 2$ and $2 > rn'_{0h}/n_{0h} > 3rT'_h/2T_h$ along with $\gamma > d$. Recall the from Eq. (49) for $rn'_{0h}/n_{0h} < 0$ we need to keep $3rT'_h/2T_h > rn'_{0h}/n_{0h}$ along with $\gamma > d$ and $\gamma\beta_b \sim 2$ to allow positive hot electron pressure gradients.

V. APPLICATIONS

As a specific application of the results obtained in the previous section we consider a hard core Z pinch as a crude approximation to a dipole with a levitated current carrying superconducting coil as in LDX. Assuming power law profiles satisfying pressure balance gives

$$B_0 = B_a \left(\tfrac{a}{r}\right)^{1/(1+\beta)} \text{ and } p_0 = p_a \left(\tfrac{a}{r}\right)^{2/(1+\beta)}, \tag{50}$$

where a is the radius of the current carrying hard core conductor, B_a and p_a are the magnetic field and total plasma pressure at its surface, respectively, and $\beta = 2\mu_0 p_a / B_a^2$ is the total beta. If we assume that the background and hot pressure profiles are the same, then $p_a = p_{ab} + p_{ah}$ with $p_{ab} \sim p_{ah}$ and

$$p_{0b} = p_{ab} \left(\tfrac{a}{r}\right)^{2/(1+\beta)} \text{ and } p_{0h} = p_{ah} \left(\tfrac{a}{r}\right)^{2/(1+\beta)}, \tag{51}$$

where $\beta = 2\mu_0 (p_{ab} + p_{ah})/B_0^2 = \beta_b + \beta_h$.

For this special model

$$s = -\frac{\beta r p_0'}{2 p_0} = \frac{\beta}{(1+\beta)} > 0 \text{ and } s_h = -\frac{\beta_h r p_{0h}'}{2 p_{0h}} = \frac{\beta_h}{(1+\beta)} > 0. \tag{52}$$

Note that since $s < 1$, drift reversal is not possible in this model. The stability condition for a hard core Z-pinch with the above profiles can be obtained by substituting these expressions for s and s_h into the lowest order dispersion relation, Eq. (32), to find

$$\frac{\omega^2}{\omega_{\kappa e}^2} = \left(\frac{rV'}{V}\right)^2 \frac{(\gamma-d)}{b} \frac{\left(1+\frac{1}{2}d\beta_b+\frac{\beta_h}{1+\beta}I\right)}{\left(1+\frac{1}{2}\gamma\beta_b+\frac{\beta_h}{1+\beta}I\right)}, \tag{53}$$

where $d = 2/(2+\beta) > 0$ and $[1 + d\beta_b/2 + \beta_h I/(1+\beta)]/[1 + \gamma\beta_b/2 + \beta_h I/(1+\beta)] > 0$ since $I > 0$. Therefore, in the absence of resonant hot electron effects the stability boundary is described by

$$\gamma > d = \frac{2}{2+\beta}, \tag{54}$$

which is always satisfied.

To determine the stability condition for the case of $\beta_h \gg \beta_b$, we assume power law temperature and density profiles

$$T_h = T_{ah} \left(\frac{a}{r}\right)^{q_h/(1+\beta)} \text{ and } n_{0h} = \frac{p_{ah}}{T_{ah}} \left(\frac{a}{r}\right)^{(2-q_h)/(1+\beta)} \tag{55}$$

with $0 < q_h < 2$. Substituting the expressions for s and s_h along with the hot electron number density gradient into Eq. (38), we find the stability condition to be the same as in the $\beta_h \sim \beta_b$ case. For $\beta_b \to 0$ Eq. (38) is satisfied since $1 + Y > 0$. For the case of $\beta_b \neq 0$, Y is smallest if $b = 0$. Moreover, a plot of $1 + Y$ as a function of β_b/β in Fig. 4 for different values of q_h and $\gamma\beta_b = 3$ always finds $1 + Y > 0$ (note that since $\beta = \beta_b + \beta_h$ we have $0 \leq \beta_b/\beta \leq 1$). For other

values of $\gamma\beta_b$ the plots look very similar to Fig. 4 and thus, even for the worst case of $b = 0$, Eq. (38) is satisfied.

To determine the effects of a resonant hot electron population on the stability, we note that due to Eq. (55), the hot number density is monotonically decreasing, $rn'_{0h}/n_{0h} < 0$, and therefore $H > 0$. Since $d < \gamma$, K is positive either due to $\alpha > 1$ or $0 < \alpha < 1$ and thus $1 + H\alpha/(1 - \alpha) > 1$. Therefore, for $\beta_h \sim \beta_b$ or $\beta_h \gg \beta_b$ the stability is determined by the sign of Δ so this hard core Z-pinch will remain stable if $\eta_h > 2/3$ or $q_h > 4/5$.

Finally, we remark that if the unperturbed hot electron distribution function is simply assumed to be a drifting Maxwellian, then from Eq. (19) we find the flow $\vec{\mathbf{v}}_h = \hat{\mathbf{z}}(T_h n'_{0h}/m\Omega_e n_{0h})$ along with the restriction that $\nabla T_h = 0 = \eta_h$. As a result, for this "rigid rotor" equilibrium case, even though $s < 1$, a weak resonant hot electron driven instability always occurs.

VI. CONCLUSION

The effects of hot electrons on the interchange stability of a Z-pinch plasma are investigated. The results yield two types of different resonant hot electron effects that modify the usual ideal MHD interchange stability condition.

Our analysis indicates that when the magnetic field is an increasing function of radius, there is a critical pitch angle for which the magnetic drift of hot electrons reverses direction. The interaction of the wave and the particles with the pitch angles close to critical always causes instability. Thus, stable operation is not possible when the magnetic field increases with radius.

If drift reversal ($s < 1$) does not occur and resonant hot electron effects are neglected, we find that interchange stability remains robust and is enhanced by increasing the background plasma pressure as well as the gradient of the hot electron density for $\beta_h \gg \beta_b$ case. However, once β_b becomes of order two or three, further increases in β_b do not result in significant increases in stability. In the absence of drift reversal, hot electron effects are weak, but not negligible. When they are retained, an additional constraint must be satisfied to avoid a weak resonant hot electron instability. For $\beta_h \sim \beta_b$ and under certain conditions for $\beta_h \gg \beta_b$, the hot electron density and temperature profiles must satisfy $r n'_{0h} / n_{0h} > 3 r T'_h / 2 T_h$. For the important case of $\beta_h \gg \beta_b$, no simple constraint can be found. However, numerical calculations suggest that keeping $\gamma \beta_b \sim 2$, $r n'_{0h} / n_{0h} \sim 1$, and the hot electron fraction high yields the largest stable operating regime. Stability in the electrostatic limit ($\beta_b = 0$) is particularly awkward since it requires $r n'_{0h} / n_{0h} > 3 r T'_h / 2 T_h$ with no peak in the hot electron pressure profile.

The effect of a hot electron population on Z pinch stability is motivated by a desire to determine what physical mechanism must be accounted for when the stability of a dipole confined plasma is investigated in the presence of electron cyclotron heating. Our study has demonstrated the key roles that hot electron magnetic drift reversal and the hot electron fraction and profiles will play in the Levitated Dipole Experiment.

ACKNOWLEDGMENTS:

APPENDIX: EVALUATION OF HOT ELECTRON RESPONSE EXPRESIONS.

This appendix presents details of hot electron response expressions G, H and $s_h I$. Recall that the perturbed hot electron density and radial current are given by

$$\frac{n_{1h}}{n_{0h}} = \frac{1}{n_{0h}} \int f_{1h} d\vec{\mathbf{v}} = \frac{e\Phi}{T_h} G + \frac{B_{1\theta}}{B_0} H \tag{A1}$$

and

$$\frac{\mu_0 J_{1hr}}{ikB_0} = -\frac{\mu_0 e}{ikB_0} \int \mathbf{v}_r f_{1h} d\vec{\mathbf{v}} = \frac{e\Phi_1}{T_h}\frac{\beta_h}{2} H - \frac{B_{1\theta}}{B_0} s_h I , \tag{A2}$$

with f_{1h} given by Eq. (26). Thus, the expressions for G, H and $s_h I$ can be written as

$$G = 1 - \frac{2\omega_{*h}}{\sqrt{\pi}\omega_{\kappa h}} \int\limits_0^\infty dt e^{-t^2} \left[1 + \eta_h\left(t^2 - \frac{3}{2}\right)\right] \int\limits_{-1}^1 \frac{d\lambda}{D - \omega/\omega_{\kappa h}t^2} , \tag{A3}$$

$$H = \frac{2\omega_{*h}}{\sqrt{\pi}\,\omega_{\kappa h}} \int\limits_0^{\infty} dt\, e^{-t^2} t^2 \left[1 + \eta_h\left(t^2 - \frac{3}{2}\right)\right] \int\limits_{-1}^{1} \frac{d\lambda\left(1-\lambda^2\right)}{D - \omega/\omega_{\kappa h} t^2}, \tag{A4}$$

and

$$s_h I = \frac{2\omega_{*h}}{\sqrt{\pi}\,\omega_{\kappa h}} \int\limits_0^{\infty} dt\, e^{-t^2} t^4 \left[1 + \eta_h\left(t^2 - \frac{3}{2}\right)\right] \int\limits_{-1}^{1} \frac{d\lambda\left(1-\lambda^2\right)^2}{D - \omega/\omega_{\kappa h} t^2}, \tag{A5}$$

where $t^2 = m\mathrm{v}^2/2T_h$ and $D = (1+s)\lambda^2 + (1-s)$.

For $s < 1$ no drift reversal is possible and we can drop the $\omega/\omega_{\kappa h} t^2$ term in the denominator due to $\omega << \omega_{\kappa h}$, except for very small t, where slow electrons are resonant with the wave. Retaining this weak resonant effect the expressions for G, H and $s_h I$ become

$$G = 1 - \frac{\omega_{*h}(1-\eta_h)}{\omega_{\kappa h}} \int\limits_{-1}^{1} \frac{d\lambda}{D} + G_{res}, \tag{A6}$$

$$H = \frac{\omega_{*h}}{2\omega_{\kappa h}} \int\limits_{-1}^{1} \frac{d\lambda\left(1-\lambda^2\right)}{D} + H_{res}, \text{ and} \tag{A7}$$

$$s_h I = \frac{3\omega_{*h}(1+\eta_h)}{4\omega_{\kappa h}} \int\limits_{-1}^{1} \frac{d\lambda\left(1-\lambda^2\right)^2}{D} + s_h I_{res}, \tag{A8}$$

with

$$G_{res} = -i\frac{\sqrt{\pi}\,\omega_{*h}\left(1-\frac{3}{2}\eta_h\right)}{\omega_{\kappa h}}\sqrt{\frac{\omega}{\omega_{\kappa h}}} \int\limits_{-1}^{1} \frac{d\lambda}{D^{3/2}}, \tag{A9}$$

$$H_{res} = i\frac{\sqrt{\pi}\,\omega_{*h}\left(1-\frac{3}{2}\eta_h\right)}{\omega_{\kappa h}}\left(\frac{\omega}{\omega_{\kappa h}}\right)^{3/2} \int\limits_{-1}^{1} \frac{d\lambda\left(1-\lambda^2\right)}{D^{5/2}}, \text{ and} \tag{A10}$$

$$\left(s_h I\right)_{res} = i\frac{\sqrt{\pi}\,\omega_{*h}\left(1-\frac{3}{2}\eta_h\right)}{\omega_{\kappa h}}\left(\frac{\omega}{\omega_{\kappa h}}\right)^{5/2} \int\limits_{-1}^{1} \frac{d\lambda\left(1-\lambda^2\right)^2}{D^{7/2}}. \tag{A11}$$

Observe that since D does not vanish for $s < 1$, integrals over λ are easily evaluated, confirming that the non-resonant parts of expressions for G, H and $s_h I$ are all of order unity.

As we noted at the beginning of Sec. IV, only the non-resonant part of $s_h I$ matters in the dispersion relation for $s < 1$ to lowest order. Thus, ignoring the weak resonant effects, the hot electron response for $s < 1$ is described only by $s_h I$, where I is given by

$$I \approx \begin{cases} \frac{-1}{(1+s)^2}\left[(4+s)-\frac{3}{\sqrt{1-s^2}}\ln\left(\sqrt{s^2-1}-s\right)\right] & s < -1 \\ \frac{2}{5} & s = -1 \\ \frac{-1}{(1+s)^2}\left[(4+s)-\frac{6}{\sqrt{1-s^2}}\arctan\sqrt{\frac{1+s}{1-s}}\right] & -1 < s < 1 \end{cases}. \tag{A12}$$

(Notice for the special case of $s = -1$, D reduces to $D = 2$).

The weak resonant effect of hot electrons for $s < 1$ is calculated by evaluating the λ integrals in G_{res}, H_{res} and $(s_h I)_{res}$ to obtain the expressions given in Eqs. (40) – (41).

For $s > 1$ there is always a critical pitch angle $|\lambda_0| < 1$ for which D vanishes and therefore we must keep the ω term with $\mathrm{Im}\,\omega > 0$ to satisfy causality. Evaluating the λ integral in the expression $s_h I$, Eq. (A8), we find

$$\int_{-1}^{1}\frac{d\lambda\left(1-\lambda^2\right)^2}{D-\omega/\omega_{\kappa h}t^2} = -\frac{4}{3(1+s)^2}\left[(4+s)-3\int_{-1}^{1}\frac{d\lambda}{D-\omega/\omega_{\kappa h}t^2}\right] =$$
$$= -\frac{4}{3(1+s)^2}\left\{(4+s)-3\left[-\frac{1}{\sqrt{s^2-1}}\ln\left(s+\sqrt{s^2-1}\right)+\frac{\pi i}{2\sqrt{s^2-1}}\right]\right\}, \tag{A13}$$

where we have dropped $i\omega/\omega_{\kappa h}t^2$ order terms since they are much smaller than the leading imaginary term. As a result, for $s > 1$ we find

$$I = \frac{-1}{(1+s)^2}\left\{(4+s)+\frac{3}{\sqrt{s^2-1}}\ln\left(s+\sqrt{s^2-1}\right)-\frac{3\pi i}{2\sqrt{s^2-1}}\right\}. \tag{A14}$$

Finally, we have to evaluate the expression for I at $s \rightarrow 1$. The vicinity of $s = 1$ is the only region were the ω and t dependence of the integral

$$\int_{-1}^{1} \frac{d\lambda}{D-\omega/\omega_{\kappa h}t^2} \underset{s\to 1}{\approx} \begin{cases} \dfrac{\pi}{\sqrt{2\left(1-s-\omega/\omega_{\kappa h}t^2\right)}}-1\ldots & s<1 \\[4mm] \dfrac{\pi i}{\sqrt{2\left(s-1+\omega/\omega_{\kappa h}t^2\right)}}-1\ldots & s>1 \end{cases} \tag{A15}$$

enters. The weak t dependence makes it awkward to do the t integrals exactly. However, to get the region about $s=1$ approximately correct, we evaluate the integrals in $s_h I$ at $s=1$ getting

$$I = -\left[\frac{5}{4}-i\sqrt{\frac{\omega_{\kappa h}}{\omega}}\,\frac{\sqrt{2\pi}\left(1+\frac{3}{2}\eta_h\right)}{(1+\eta_h)}\right], \tag{A16}$$

and then use the result to make an approximate fit that is independent of t. This procedure is equivalent to making the replacement

$$\int_{-1}^{1} \frac{d\lambda}{D-\omega/\omega_{\kappa h}t^2} \underset{s\to 1}{\to} \begin{cases} \dfrac{\pi}{\sqrt{2(1-s-\sigma\omega/\omega_{\kappa h})}}-1\ldots & s<1 \\[4mm] \dfrac{\pi i}{\sqrt{2(s-1+\sigma\omega/\omega_{\kappa h})}}-1\ldots & s>1, \\[4mm] \dfrac{\pi i}{\sqrt{2\sigma\omega/\omega_{\kappa h}}}-1\ldots & s=1 \end{cases} \tag{A17}$$

where

$$\sigma = \left[\frac{3(1+\eta_h)}{4\sqrt{\pi}(2+3\eta_h)}\right]^2.$$

Notice that if we were to repeat the same procedure for G and H as given by Eqs. (A3) – (A4) for $s>1$ and $s\to 1$, we would find that they are of the same order as $s_h I$ and therefore would not be significant in the dispersion relation.

REFERENCES

[1] A. Hasegawa, Comments on Plasma Phys. Controlled Fusion **1**, 147 (1987).

[2] J. Kesner, L. Bromberg, M. E. Mauel and D. T. Garnier, *17th IAEA Fusion Energy Conference, Yokahama, Japan, 1998 (International Atomic Energy Agency, Vienna, 1999)*, Paper IAEA-F1-CN-69-ICP/09.

[3] I. B. Bernstein, E. A. Frieman, M. D. Kruskal and R. M. Kulsrud, *Proc. Roy. Soc.* London, Ser. A **244**, 17 (1958).

[4] D. Garnier, J. Kesner, M. Mauel, Phys. Plasmas **6**, 3431 (1999).

[5] A. N. Simakov, P.J. Catto, S.I. Krasheninnikov and J. J. Ramos, Phys. Plasmas **7**, 2526 (2000).

[6] J. Kesner, A. N. Simakov, D. T. Garnier, P.J. Catto, R. J. Hastie, S.I. Krasheninnikov, M. E. Mauel, T. Sunn Pedersen and J. J. Ramos, Nucl. Fusion **41**, 301 (2001).

[7] A. Hansen, D. Garnier, J. Kesner, M. Mauel and A. Ram, in *Proceedings of the 14th Topical Conference on Radio Frequency Power in Plasmas* (AIP Conf. Proceedings No. 595), edited by S. Bernanei and F. Paoletti (American Institute of Physics, New York, 2001) p. 362.

[8] D. B. Nelson, Phys. Fluids **23**, 1850 (1980).

[9] C.Z. Cheng, Fusion Tech. **18**, 443 (1990).

[10] M. J. Gerver and B. G. Lane, Phys. Fluids **29**, 2214 (1986).

[11] A. N. Simakov, R. J. Hastie and P.J. Catto, Phys. Plasmas **9**, 201 (2002).

[12] T. M. Antonsen and B. Lane, Phys. Fluids **23**, 1205 (1980).

[13] P.J. Catto, W. M. Tang and D. E. Baldwin, Plasma Physics **23**, 639 (1981).

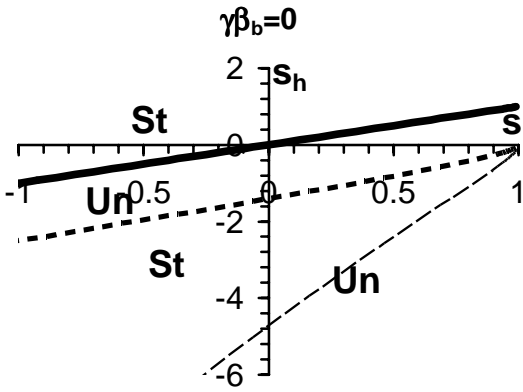[14] J.P. Freidberg, *Ideal Magnetohydrodynamics* (Plenum, New York, 1987).

FIGURE CAPTIONS

Figs. 1 (a)-(c). Stability regions for different values of $\gamma\beta_b$ with b=0.01 and $n_{0h}T_e/p_{0b}$=5%. The solid line is γ=d, dashed is $1+d\beta_b/2+s_hI$=0, and dotted is $1+\gamma\beta_b/2+s_hI$=0. St and Un indicate stable and unstable regions.

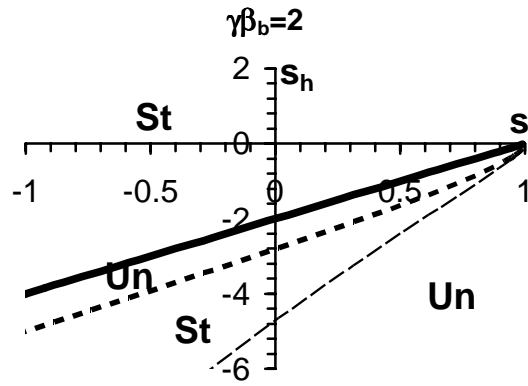Figs. 2 (a)-(d). Stability regions for different values of $\gamma\beta_b$ and rn'_{0h}/n_{0h} with b=0.01 and $n_{0h}T_e/p_{0b}$=10%. The dotted line is the $1+\gamma\beta_b/2+s_hI$=0 curve and for small $\gamma\beta_b$ the solid line approaches γ=d. The dashed line $1+d\beta_b/2+s_hI$=0 becomes as $n_{0h}\rightarrow 0$

Figs. 3 (a)-(d). Stability regions for different values of $\gamma\beta_b$ and rn'_{oh}/n_{oh} with $n_{oh}T_e/p_{0b}$=10%. The solid curve is the unstable boundary for b=0.01, the dash-dotted line is the boundary for b=0, and the doted line in (b) is an analytical approximation to b=0 curve. If only the solid line is shown, the region s_h>0 is stable for b=0 and our approximation Eq. (49) is not valid because Y~1. The faint gray curves are the lowest order boundaries as shown in Figs. 2.

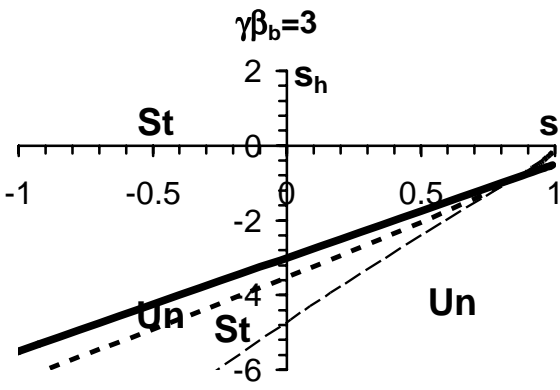Fig. 4 Graph of 1+Y vs. β_b/β for different values of q_h.

(a)

(b)

(c)

Figure 1

N.S. Krasheninnikova, P.J. Catto

γβ$_b$=2; rn'$_{0h}$/n$_{0h}$=1

S$_h$

St

Un

St

Un

s

(a)

γβ$_b$=2; rn'$_{0h}$/n$_{0h}$=-1

S$_h$

St

Un

St

Un

s

(b)

γβ$_b$=3; rn'$_{0h}$/n$_{0h}$=1

S$_h$

St

Un

St

Un

s

(c)

γβ$_b$=3; rn'$_{0h}$/n$_{0h}$=-1

S$_h$

St

Un

St

Un

s

(d)

Figure 2

N.S. Krasheninnikova, P.J. Catto

35

γβ$_b$=2; rn'$_{0h}$/n$_{0h}$=1

s$_h$

Un

s

γβ$_b$=2; rn'$_{0h}$/n$_{0h}$=3

s$_h$

Un

s

(a)

(b)

γβ$_b$=3; rn'$_{0h}$/n$_{0h}$=1

s$_h$

Un

s

γβ$_b$=3; rn'$_{0h}$/n$_{0h}$=3

s$_h$

Un

s

(c)

(d)

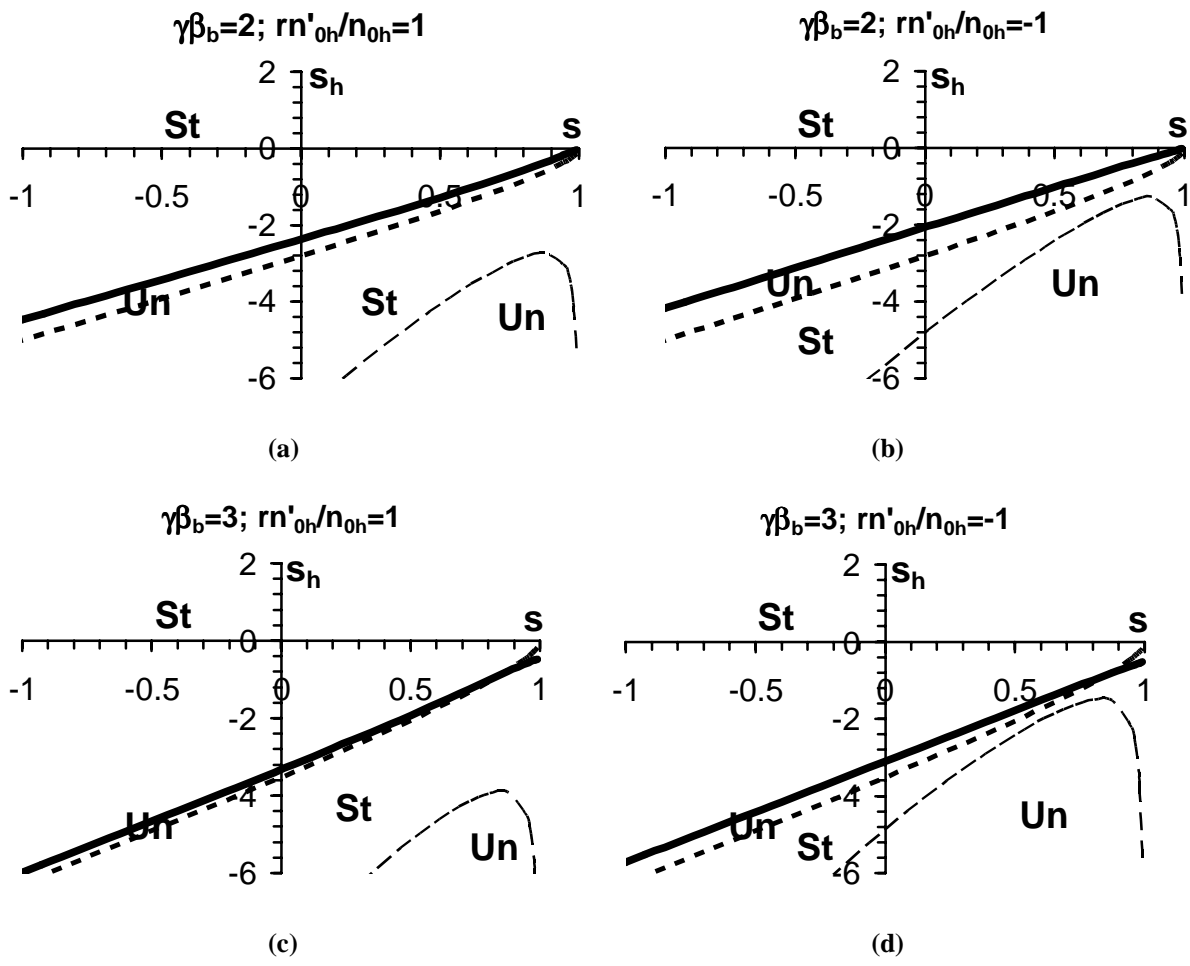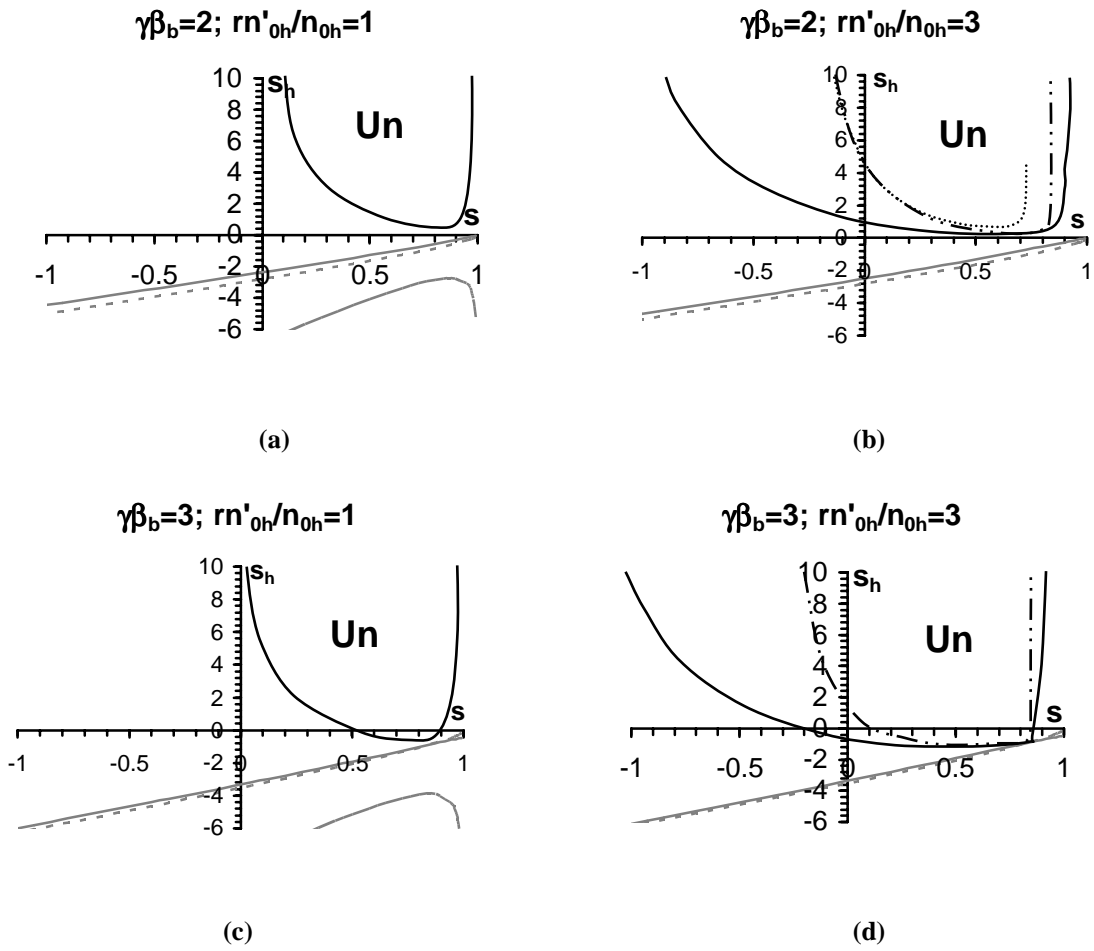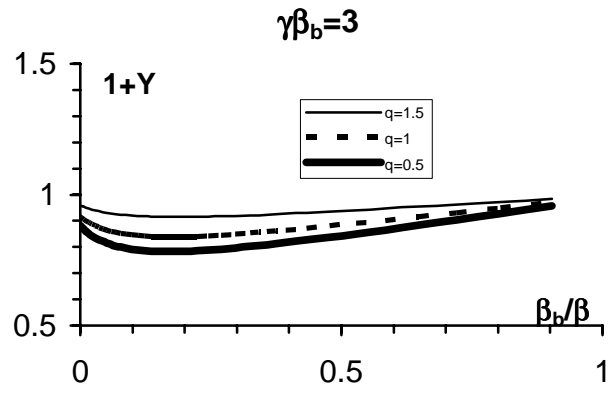**Figure 3**

N.S. Krasheninnikova, P.J. Catto

Figure 4

N.S. Krasheninnikova, P.J. Catto